AIAA JOURNAL
Vol. 32, No. 4, April 1994

# Time and Flow-Direction Responses of Shear-Stress-Sensitive Liquid Crystal Coatings

Daniel C. Reda,* Joseph J. Muratore Jr.,† and James T. Heineck‡
*NASA Ames Research Center, Moffett Field, California 94035*

**Time and flow-direction responses of shear-stress-sensitive liquid crystal coatings were explored experimentally. For the time-response experiments, coatings were exposed to transient, compressible flows created during the startup and off-design operation of an injector-driven supersonic wind tunnel. Flow transients were visualized with a focusing schlieren system and recorded with a 1000 frame/s color video camera. Liquid crystal responses to these changing-shear environments were then recorded with the same video system, documenting flow-visualization response times equal to, or faster than, the time interval between sequential frames (i.e., 1 ms). For the flow-direction experiments, a planar test surface was exposed to equal-magnitude and known-direction surface shear stresses generated by both normal and tangential subsonic jet-impingement flows. Under shear, the sense of the angular displacement of the liquid crystal dispersed (reflected) spectrum was found to be a function of the instantaneous direction of the applied shear. This technique thus renders dynamic flow reversals or flow divergences visible over entire test surfaces at image recording rates up to 1 kHz. Extensions of the technique to visualize relatively small changes in surface shear stress direction appear feasible.**

## Nomenclature

| | |
|---|---|
| $A$ | = fixed tangential jet |
| $B$ | = transversely movable jet |
| $C$ | = camera position |
| $L$ | = light source position |
| $M$ | = Mach number |
| $P_0$ | = stagnation pressure |
| $Re$ | = Reynolds number/ft |
| $Re_D$ | = Reynolds number based on jet diameter |
| $\alpha_C$, $\alpha_L$ | = camera or light angle in plane perpendicular to test surface, measured positive upwards from zero in plane of test surface |
| $\Delta$ | = change in |
| $\phi_C$, $\phi_L$ | = camera or light circumferential angle in plane of test surface, measured positive counterclockwise from origin shown in Fig. 6 |

## Introduction

IN fluid mechanics and aerodynamics research, valuable information can be gained from visualization of dynamic surface shear stress patterns on solid bodies immersed in fluid streams. The liquid crystal coating method is a diagnostic technique that can provide areal visualizations of instantaneous shear stress distributions on surfaces in dynamic flowfields with a response that is rapid, continuous, and reversible. In the present research, results have been obtained that extend the time response of this technique (for flow visualization) to order 1 ms, and, for the first time, document the shear stress direction-manifestation capabilities of the technique.

Cholesteric liquid crystals are a highly anisotroptic mesophase that exists between the solid and isotropic-liquid phases of some organic compounds.[1,2] Such materials can exhibit birefringent optical properties characteristic of a crystalline (solid) state. Once aligned by shear, molecules within a thin liquid crystal coating selectively scatter incident white light as a spectrum of colors, each color at a discrete angle (orientation) relative to the surface. For thermochromic liquid crystal compounds, in the absence of contaminants and electromagnetic fields, the aligned molecular structure, and thus the light-scattering capability of the coating, responds to both temperature and shear stress.[3] For the newly formulated, shear-stress-sensitive and temperature-insensitive compounds,[4,5] color play (i.e., discerned color changes at a fixed angle of observation, for a fixed angle of illumination) results solely from the application of shear stress. The evolution of this technique, for aerodynamic applications, can be ascertained in the writings of Klein,[6] Klein and Margozzi,[7] Holmes et al.,[8] Reda,[9] Gaudet and Gell,[10] Bonnett et al.,[11] Toy et al.,[12] Mee et al.,[13] Reda,[14] Hall et al.,[15] Parmar,[16] Toy et al.,[17] Reda and Aeschliman,[18] and Smith.[19]

While it is now known that the technique can be calibrated (under carefully controlled conditions) to measure surface shear stress magnitudes (Refs. 10–12, 16, and 17) two important issues remain: time response and directional sensitivities (to illumination and viewing angles, as well as to the instantaneous shear stress direction).

Parmar[16] investigated the time-response issue by placing a liquid crystal layer (~100 μm thick) between two optical glass plates and applying known/transient shear forces via a displacement of one plate. Liquid crystal time constants were measured as a function of the monochromatic wavelength of the incident light. Time constants in the range 10–100 ms were generally observed, with minimum values being order 3 ms. The extrapolation (or applicability) of these results to actual fluid mechanic applications, wherein liquid crystal coating thicknesses are an order of magnitude less, remains an open question.

Another approach to characterizing the time-response and/or flow-direction-indication capabilities of the liquid crystal technique is to expose the coating to transient viscous flows of known time scales and/or known shear directions. The oscillating airfoil experiments of Reda[9,14] provided some initial results concerning both issues. New results are presented in subsequent sections.

## Coating Application Technique

In flow-visualization applications, a mixture of one part liquid crystals to nine parts solvent (presently, Freon) is sprayed onto the

Presented as Paper 93-0183 at the AIAA 31st Aerospace Sciences Meeting, Reno, NV, Jan. 11–14, 1993; received Jan. 18, 1993; revision received June 11, 1993; accepted for publication June 21, 1993. 

*Senior Research Scientist, Fluid Mechanics Laboratory Branch, MS:260-1. Associate Fellow AIAA.

†Research Assistant, MCAT Institute, MS:260-1.

‡Scientific and Technical Photographer, Imaging Technology Branch, MS:203-6.

aerodynamic surface under study. For small test areas, an artist airbrush is the preferred spray tool. A smooth, flat-black surface is essential for color contrast and must be kept free of grease and other chemical contaminants. Recommended applications (after spray losses) are 10–20 ml liquid crystals, measured prior to mixing with the solvent, to each square meter of surface area. The solvent evaporates, leaving a uniform thin film of liquid crystals whose thickness, based on mass conservation and estimated spray losses, is approximately 10–20 μm (0.0004–0.0008 in.). The molecules within the as-sprayed coating are generally not aligned into the planar texture required to disperse white light into a spectrum.

## Time Response

The time response issue was further investigated by exposing coatings of a newly formulated, shear-stress-sensitive/temperature-insensitive liquid crystal compound[4] (Hallcrest BCN/192) to transient, compressible flows created during the startup and off-design operation of an injector-driven supersonic wind tunnel[20] (see schematic, Fig. 1).

In this facility, supersonic injector flows ($P_0$ = 1 atm, $M$ = 2.4, $Re = 9.8 \times 10^6$/m) emanating from above and below the supersonic diffuser exit were used to pull the primary flow through the nozzle

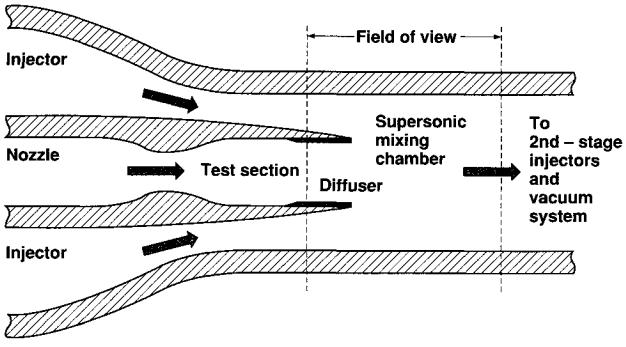


**Fig. 1 Schematic of injector-driven supersonic wind tunnel.**

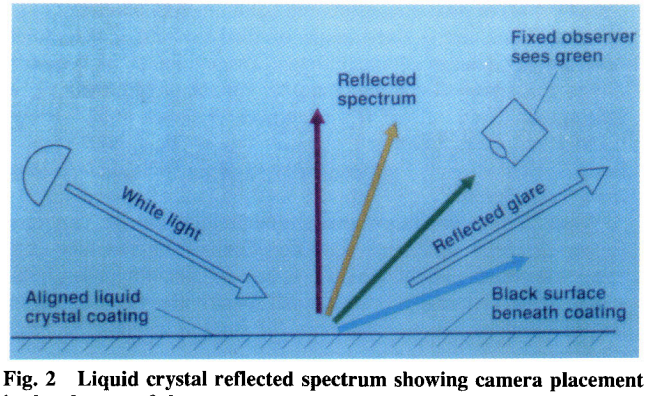


**Fig. 2 Liquid crystal reflected spectrum showing camera placement in the absence of shear.**

($P_0$ = 0.35 atm, $M$ = 2.5, $Re = 3.3 \times 10^6$/m); the three merged streams then flowed to a downstream reservoir maintained at 0.55 atm by a vacuum compressor. During these tests, all boundary layers on the tunnel sidewall surfaces were turbulent and the settling chamber was completely open (i.e., no noise or turbulence suppression devices were installed). Transient flowfield events (unsteady shock wave/boundary-layer interactions and supersonic shear layer unsteadiness) responsible for generating transient surface shear stress distributions on the tunnel sidewall (within the field of view delineated in Fig. 1) were documented in precursor experiments using a focusing schlieren system and a high-speed NAC HSV-1000 video camera (to 1000 frames/s). Observable mean-flow transients of time scales ≤ 1 ms were found to be present.

For the liquid crystal experiments, one sidewall window of the tunnel was removed and replaced with a solid (black) flush-mounted metal insert, which became the test surface. The visible surfaces beneath the three separate streams, and the surface area within the mixing region immediately downstream of the injector/diffuser exit plane, were obliquely illuminated by white light (5600 K with a flicker-free ballast) from the downstream direction (i.e., the principal flow direction was towards the light). The angle of illumination was approximately 45 deg from the sidewall plane.

Initial attempts at viewing and recording the liquid crystal color-play response were made on a line of sight perpendicular to the test surface. Under these conditions, essentially no color play could be observed. Post-test observations of the shear-aligned liquid crystal coating showed that the spectrum of scattered light (under no-shear conditions) came off the surface in the upstream direction (away from the light) starting with red on the normal, yellow at approximately 30 deg from normal, green at approximately 45 deg from normal, followed by reflected glare, then turquoise (bluish-green) inside the reflected glare line (see schematic of Fig. 2).

For subsequent experiments, the recording devices (movie and/or video cameras) were positioned near the no-shear midspectrum location, i.e., just before the yellow-to-green transition angle for the shear-aligned coating. Using this camera-alignment procedure, the dynamic surface shear stress patterns on the tunnel sidewall were rendered visible in a most impressive and informative manner. Sample results (individual frames) recorded at 30 frames/s with a standard color video system are shown in Fig. 3. The total elapsed time of this tunnel startup sequence was a few seconds. Very high steady-state shear levels beneath the two injector streams caused a loss of color play to occur, i.e., the black surface beneath the coating became visible. Two plausible reasons for this observation exist: either the molecular structure was temporarily forced into an optically extinct state or the dispersed light incident on the camera was shifted outside the visible spectrum. Similar results were seen by Bonnett et al.[11] at high shear rates. Upon removal of shear stress, the entire coating returned to its aligned (color-play) state.

Liquid crystal coating color-play response was also recorded using the NAC Visual Systems HSV-1000 high-speed color video system. Liquid crystal coating response time to shear was documented to be equal to, or less than, the time interval between

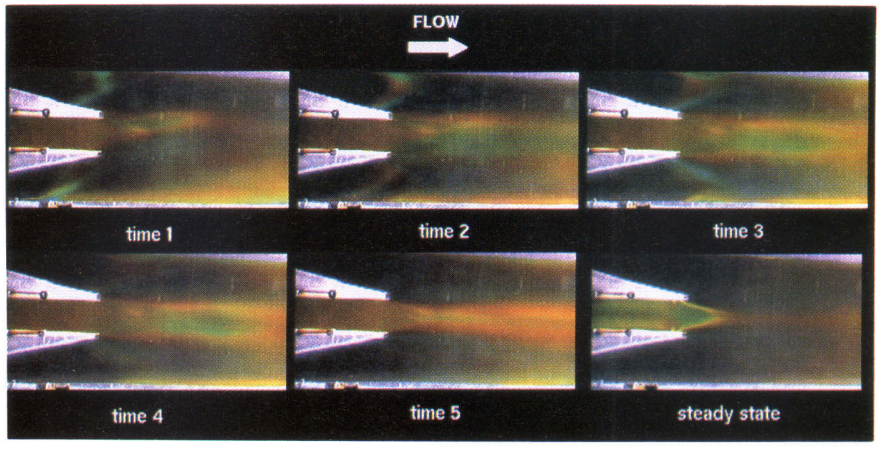


**Fig. 3 Liquid crystal color patterns during tunnel startup.**

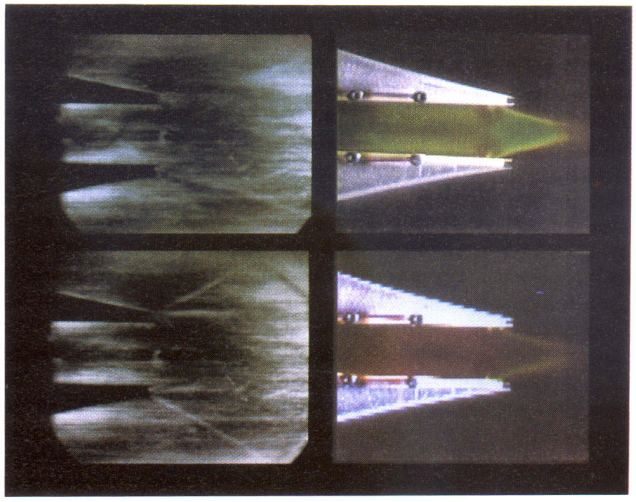

**Fig. 4 Schlieren and liquid crystal images: top line, diffuser started; bottom line, diffuser unstarted.**

sequential frames recorded at 1 kHz, i.e., 1 ms. A color video summarizing these observations is available to interested researchers (request AAV #1373, 9/91). It is also interesting to note that recent research[21,22] into the time response of liquid crystal displays (i.e., the transmission of light through liquid crystal layers exposed to impulsively changed electric fields) has shown achievable liquid crystal response times to be an order of magnitude faster (~0.1 ms).

Results obtained during the present experiments also showed that when the nozzle flow was maintained at a total pressure just below the established minimum-run value of ~0.35 atm, random unstarts and restarts of the supersonic diffuser flowfield would occur. In such instances, the shock pattern in and downstream of the diffuser, and the shear layer lateral extent within the mixing region, would all abruptly change. During these highly transient events, the liquid crystal color seen on the diffuser sidewall would also abruptly change from green to red, then red back to green (see frames in Fig. 4). Under no-shear conditions (recall Fig. 2), these two wavelengths of light (red vs green) had angular orientations on opposite sides of the recording device.

Under steady-state run conditions, reverse flows were known to exist on the supersonic diffuser sidewalls beneath the shock wave/boundary-layer interaction region. During momentary unstarts, high-velocity subsonic/attached flows most probably formed, thereby abruptly changing both the surface shear stress magnitude and direction (by 180 deg).

Figure 5 shows a two-part schematic that summarizes the apparent flow-direction-indication capabilities of the shear-aligned liquid crystal coating for the special case wherein the light, camera, and principal flow directions are all in the same plane. Further research into this aspect of liquid crystals was then initiated, and results are presented in the following sections.

## Shear-Direction Response

Based on the observations discussed previously, the following question was posed: Was the sense of the angular displacement of the dispersed (reflected) spectrum relative to a fixed observer dependent on the instantaneous direction of the shear stress vector acting on the coating? Two simple bench-top experiments were devised to answer this question, one involving a single jet of air impinging normal to a planar test surface, and the other incorporating two tangential jets of equal strength but opposite directions flowing across a planar test surface.

The experimental arrangement was as follows. Clean, dry, pressurized air was fed through two pressure regulators placed in series; output pressure was thus held constant. Air flow was then passed through a single, adjustable valve and tubing to the normal jet, or through a tee and two identical adjustable valves plus tubing (in parallel) to the tangential jets. All jet flows issued from rigid circular tubes with sharp/beveled exits of i.d. = 0.84 cm (0.33 in.) into atmospheric air. Exit velocity was approximately 76 m/s (250 ft/s) yielding $Re_D \sim 40{,}000$.

For the normal jet experiments, an overhead support frame allowed the jet exit plane to be held three jet exit diameters above the test surface. Unless otherwise noted, the normal jet stagnation point was at the center of the test surface, a flat-black 12.7 × 12.7-cm (5 × 5-in.) metal plate. For the tangential jet experiments, two separate support frames were positioned on either side of the same test surface, and the beveled jet exits were precisely set to just touch the sharp side edges of the test plate. One tangential jet could be moved laterally along its side of the test plate, allowing the opposite-direction jets to either pass by one another or to impact head on. The equal strength of the opposing jets could thus be verified by observing the mean stagnation point location and forcing it (via valve tuning) to be coincident with the plate center.

The test surface was always cleaned and resprayed with a new liquid crystal coating (Hallcrest BCN/192) before each experiment. Molecules within the coating were always prealigned by shear into the color-play state through the oblique, multidirectional passage of a pressurized air stream over the test surface.

For the normal jet experiments, the coated test surface rested on a single-column support stand anchored into the top of an optics table. A two-degree-of-freedom, optics-traversing rig (which pivoted about both the vertical and one horizontal axes through the center of the plate) allowed the test surface to be imaged at any $\phi$, $\alpha$ combination within the quarter-spherical space encompassing the dispersed spectrum (i.e., on the side of the test surface opposite the light source). For the tangential jet experiments, two fixed/synchronized video cameras were used at symmetric angles to either

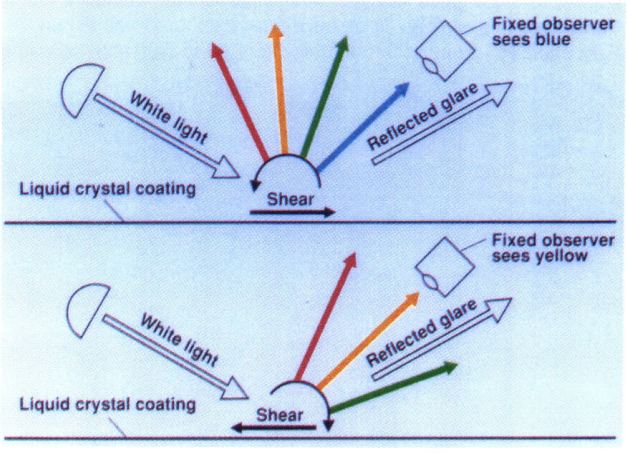


**Fig. 5 Apparent spectrum rotation as a function of shear direction for light, camera, and shear all in same plane.**

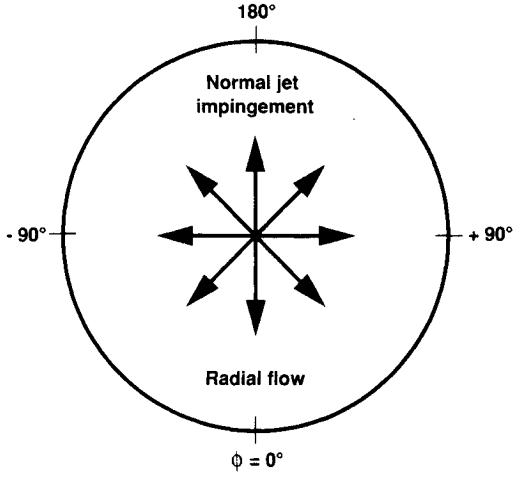


**Fig. 6 Shear vectors for circular jet impinging normal to planar surface.**

side of the light plane. In all cases, distances between the cameras and the test surface were kept large compared to the length scales under observation; long-focal-length lenses were used to ensure essentially constant view angles for all points under observation.

White light (5600 K) was supplied from a NAC Visual Systems HMI-1200 unit incorporating a 1200-W Sylvania PAR64 Brite-Beam source with an ultraviolet filter and a flicker-free ballast. The oblique lighting angle was set at $\alpha_L = 25$ deg throughout. Three-chip CCD color video cameras produced by Sony and AMPEX were utilized to capture the color images, with signals recorded in BETACAM-SP format.

A color video summarizing the flow-direction-indication experiments is also available to interested researchers (request AAV #1433, 9/92). Results of these experiments are presented in the next two sections.

### Case 1: Normal Jet Impingement

At any specified radial distance from its stagnation point, a circular jet impinging normal to a flat surface imposes an infinite number of equal-magnitude shear stress vectors on the surface, with angular orientations varying continuously from 0 to 360 deg. Such a flowfield is similar to a source flow (see schematic of Fig. 6).

Camera sweeps were made through the liquid-crystal-dispersed color space under no-shear conditions prior to recording the shear-induced color patterns for this flowfield. Results are shown in Figs. 7 and 8.

For the light source positioned at $\phi_L = 180$ deg, $\alpha_L = 25$ deg, a vertical camera sweep in the light plane ($\alpha_C$ from ~10 to ~80 deg at $\phi_C = 0$ deg) showed a progression of colors, from blue at shallow angles, through green and yellow at intermediate angles, to red at the steeper angles (Fig. 7). A horizontal camera sweep across the light plane ($\phi_C$ from $-90$ to $+90$ deg at $\alpha_C = 45$ deg) showed a different progression of colors, from red on the side, through yellow, to green in the light plane, then inverting in sequence, from green, through yellow, back to red on the other side (Fig. 8). Combined results of Figs. 7 and 8 document that the no-shear color space is, in fact, three dimensional and symmetric about the light plane.

Shear-induced color patterns beneath the normal-jet-impingement flowfield were then documented using the same horizontal camera sweep employed with Fig. 8. Results are shown in Fig. 9. A dependency of color play on shear direction was thus clearly documented: some radial shear directions caused a shift from the local no-shear color towards the blue side of the spectrum, whereas opposing shear directions caused a shift towards the red. The overall two-lobe color pattern rotated clockwise as the observer rotated counterclockwise, yielding mirror images at equal $\Delta\phi$ angles about the light plane. Changing the sense of the camera rotation changed the sense of the color pattern rotation. The perceived rotation rate of the two-lobe color pattern with changes in $\phi_C$ (in either sense), was always greatest as the observer passed through the light plane. For the special case when the camera was in the light plane (middle frame of Fig. 9), color shifts for flow away from the observer vs color shifts for flow towards the observer were found to be entirely consistent with the earlier observations of Figs. 4 and 5, i.e., the dispersed spectrum appeared to rotate towards the tail of the local shear stress vector.

Similar experiments were also conducted using the other five liquid crystal compounds listed in Refs. 4 and 5. All of these shear-stress-sensitive coatings responded in a like manner, i.e., all demonstrated a dependency of color play on shear direction. The normal-jet-impingement flowfield can thus be used to calibrate the shear-direction response of any such coating.

Experiments were then undertaken to quantify the three-dimensional color spaces shown in Figs. 7–9 (for BCN/192). The video

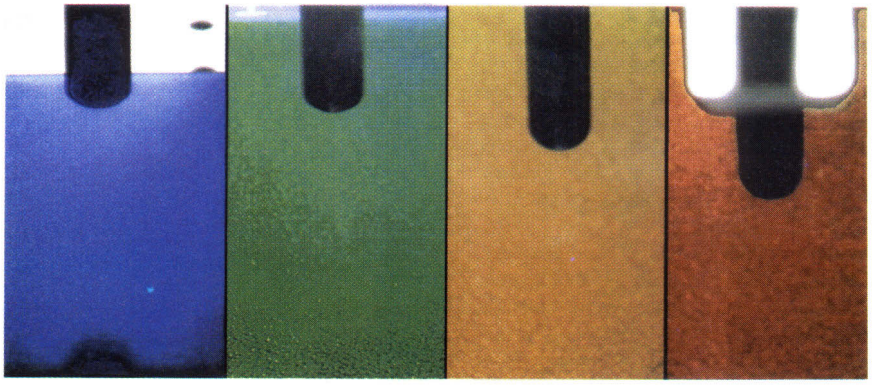

**Fig. 7 No-shear reflected colors, $\phi_C = 0$ deg, $\alpha_C$ increasing left to right.**

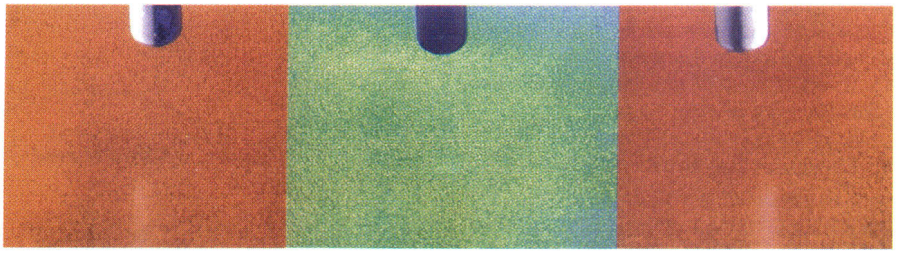

**Fig. 8 No-shear reflected colors, $\alpha_C = 45$ deg, $\phi_C = -90$, 0, and +90 deg.**

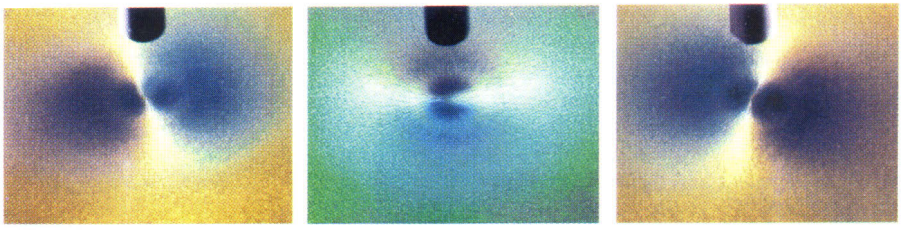

**Fig. 9 Shear-induced color patterns beneath normal jet, $\alpha_C = 45$ deg, $\phi_C = -45$, 0, and +45 deg.**

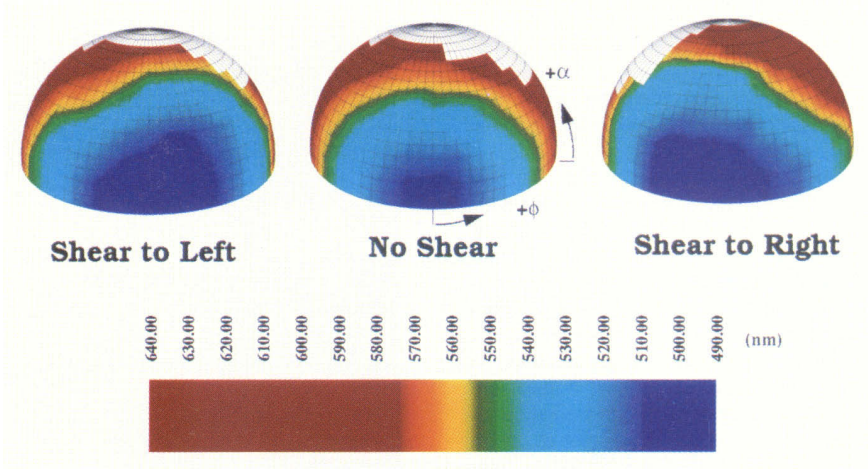


**Fig. 10 Spectrophotometer measurements of peak-power reflected wavelengths vs ϕ, α view-angle combinations in spherical space.**

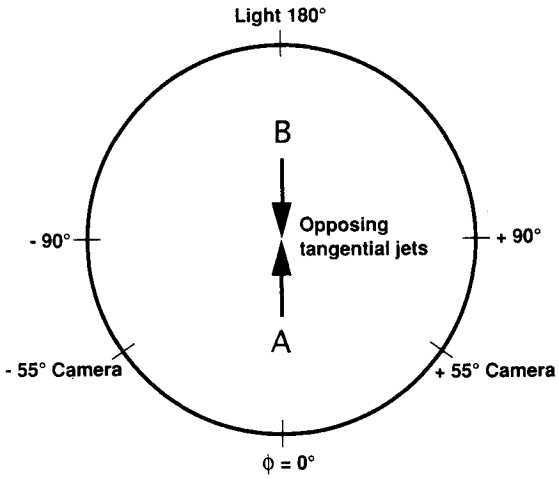


**Fig. 11 Experimental arrangement for light source aligned with opposing tangential jets.**

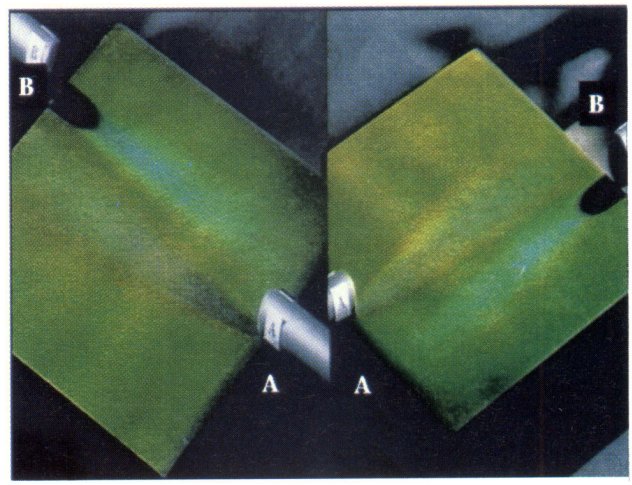


**Fig. 13 Tangential-jet-induced color patterns for Fig. 11; jets side by side.**

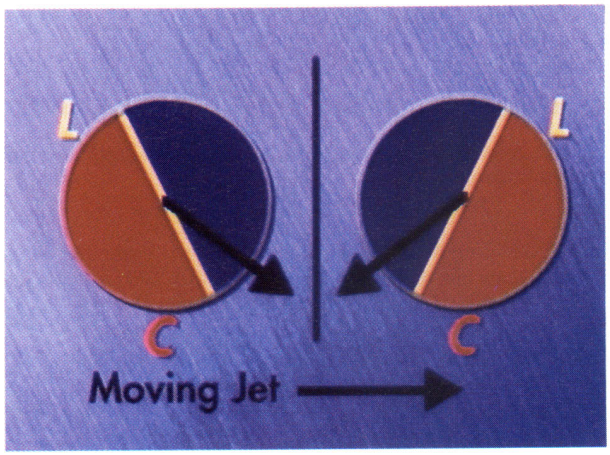


**Fig. 12 Normal-jet-impingement color patterns for symmetric views of Fig. 11; vector shows orientation of transversely movable jet *B* relative to each camera.**

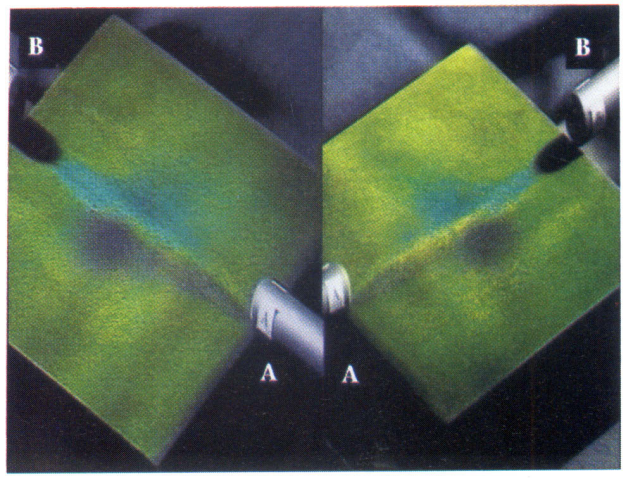


**Fig. 14 Tangential-jet-induced color patterns for Fig. 11; jets colliding head-on.**

camera was removed from the traversing rig and replaced with a 1.6-mm-diameter fiber optic bundle having a transmission bandwidth of 400–1500 nm. This probe effectively sampled scattered light only from a point at the center of the test surface (coincident with the center of rotation for the two-degree-of-freedom traversing rig). At every point on a $\Delta\phi = 10$ deg, $\Delta\alpha = 10$ deg grid, the light captured by this probe was input to a spectrophotometer (Oriel Instaspec II diode array system) which dispersed the sampled light into its spectral content, then projected it as a continuous spectrum onto a linear diode array. The output was a plot of relative light power vs wavelength. The wavelength corresponding to the peak power in each such curve was read and recorded. It should be noted that this single parameter gives an indication of the color seen by an observer at each ϕ, α position, but, by itself, does not strictly quantify the color. Given this limitation, numerical values of peak-power wavelength were assigned a color in the data analysis software such that the output color plots were consistent with the video images. Results are shown in Fig. 10 as color-coded contours of peak-power wavelength (nm) seen by an observer positioned at each point within the quarter-spherical

space containing the dispersed spectrum (the $\phi = 0$-deg line is at the front/center of each globe). A 5 × 5-deg grid is superimposed on each contour plot and data measured along the $\alpha = 10$ deg line were used to plot the unmeasurable values along the $\alpha = 0$ deg line. White portions of these plots were not viewable by the probe due to physical constraints.

Under no-shear conditions (the center plot in Fig. 10), the reflected color space was found to be three-dimensional and symmetric about the light plane, as described earlier in Figs. 7 and 8. Two additional experiments were then conducted to monitor the angular reorientations of this no-shear color space by the imposition of equal-magnitude shear stress vectors having opposite directions. Shear to the left (towards $\phi = -90$ deg) was achieved by offsetting the stagnation point of the normal jet three jet diameters to the right of the test plate center; similarly, shear to the right (towards $\phi = +90$ deg) was achieved by a three-diameter offset of the stagnation point to the left of plate center. The point of observation for the $\phi$, $\alpha$ mapping (i.e., the center of rotation for the fiber optic probe) thus remained at the plate center. Equal-magnitude/opposite-direction shear vectors at right angles to the light plane resulted in significant reorientations of the dispersed spectrum (see outside two frames of Fig. 10), but these altered color-space patterns were found to be mirror images of one another, consistent with the observations of Fig. 9.

**Case 2: Tangential Jet Impingement**

The other bench-top experiment involved the use of two equal-strength/opposite-direction tangential jets. The first of two lighting/viewing arrangements is shown in Fig. 11, where the plane of

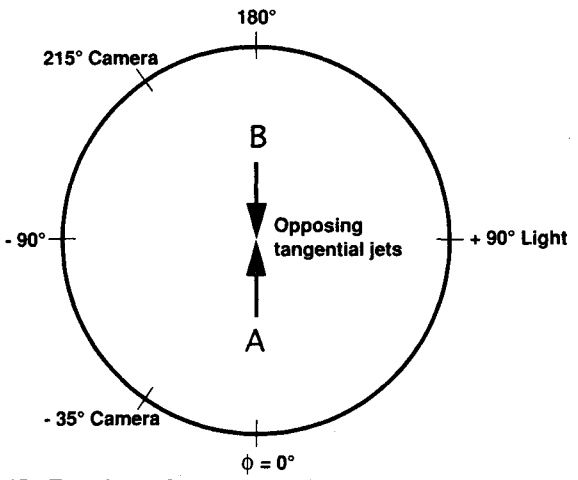


**Fig. 15 Experimental arrangement for light source perpendicular to plane of tangential jets.**

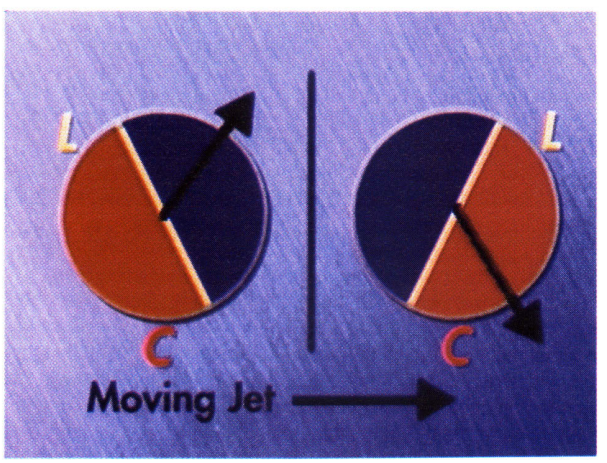


**Fig. 16 Normal-jet-impingement color patterns for symmetric views of Fig. 15; vector shows orientation of transversely movable jet *B* relative to each camera.**

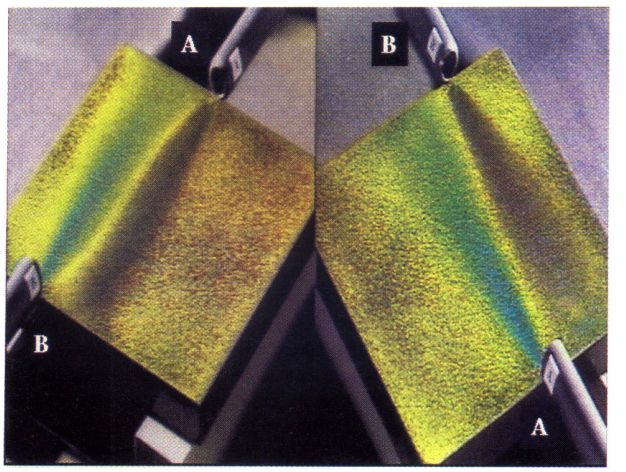


**Fig. 17 Tangential-jet-induced color patterns for Fig. 15; jets side by side.**

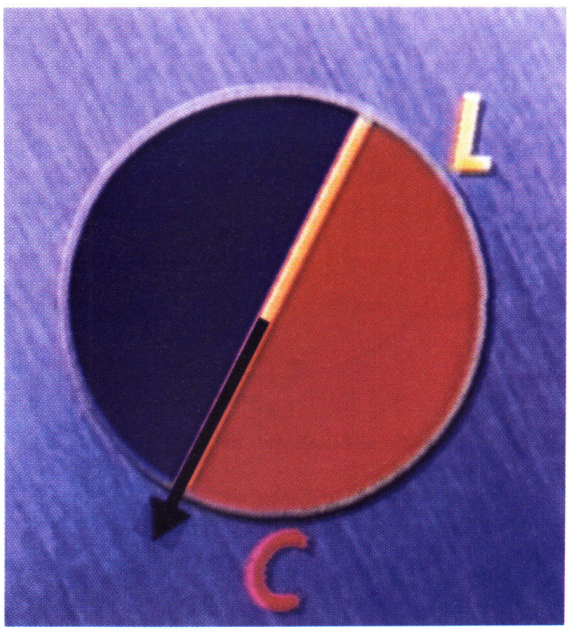


**Fig. 18 Potential extension of technique to visualize small directional changes in shear vector.**

the jets and the plane of the light source were aligned. The oblique lighting angle remained at $\alpha_L = 25$ deg for $\phi_L = 180$ deg. The fixed jet is denoted by *A* and the transversely movable jet is denoted by *B*.

The two fixed/synchronized video cameras were positioned at symmetric angles (±55 deg) to either side of the light plane, and their (matching) elevation angle was set at $\alpha_C = 30$ deg so that each camera was in a midspectrum position under no-shear conditions (see again the no-shear color space of Fig. 10).

The normal-jet-induced color patterns for these two symmetric views about the light plane are redrawn in Fig. 12. The observer *C* is at the bottom in both views to be consistent with the simultaneous video frames to be presented next. The reason for reintroducing the normal-jet color patterns is to re-emphasize the fact that such results calibrate the directional response of any liquid crystal coating. One shear vector is shown in each view, illustrating the orientation of the transversely movable jet relative to each observer. According to the shear-direction calibration, shear beneath this particular vector should induce blue in both views. Conversely, the opposite-direction, fixed-jet shear vector (not shown) should induce red in both views. Results of the actual experiment are shown in Figs. 13 and 14.

Consistent with normal-jet results, the transversely movable jet *B* induced blue in both views, while the fixed jet *A* induced red in both views (Fig. 13). The most vivid colors, however, were seen to occur in the crossflow directions (perpendicular to the light plane) experienced when the two jets collided head-on (Fig. 14).

The light plane was thus rotated to be perpendicular to the plane of the jets (Fig. 15). As before, two fixed, symmetric, and synchronized views were utilized. Once again, the normal-jet-induced color patterns for two symmetric views (±55 deg) about the light plane are redrawn (Fig. 16). As before, the observer *C* is at the bottom in both views. Under these lighting and viewing conditions, the movable jet (indicated by the single vector symbol in each view) was expected to induce blue in the left view, and, simultaneously, red in the right view. Actual results of the experiment (Fig. 17) show that this was indeed the case. Most importantly, opposite flow directions were still seen as different colors to each observer. Comparing Figs. 13, 14, and 17 demonstrates that the strongest color play (most vivid colors) occurred when the principal flow directions were at right angles to the light plane.

The answer to the question posed earlier was positive. Dynamic surface shear stress directions beneath unsteady/quasi-two-dimensional reversing or diverging (separating or reattaching) flows can now be made visible over an entire test surface at image recording rates up to order 1 kHz. Applications of this technique to unsteady attachment-line flows on the leading edges of wings also appear feasible.

A potential application of this flow-direction-indication technique, to visualize relatively small changes in surface shear stress direction, is outlined in Fig. 18. Again, relying on the normal-jet calibration, proper selection of the lighting and viewing angles could allow the principal flow direction to be aligned with the split between the two different-colored lobes. In this case, small changes in surface shear stress direction to one side of the mean-flow vector should induce a yellow-to-blue shift, whereas, conversely, a small change to the other side of the principal shear vector should induce a yellow-to-red shift.

## Future Plans

In summary, given the recent quantitative calibrations of Gaudet and Gell,[10] Bonnett et al.,[11] Toy et al.,[12,17] and Parmar[16] relating measured color changes to measured variations in surface shear stress magnitude, and taking into account the results of the present research, we can now state that liquid crystal color-change response depends on both shear stress magnitude and direction. The next challenge is to capitalize on this newly acquired knowledge to convert the liquid crystal coating technique from a visualization method into a quantitative tool for the measurement of surface shear stress vector fields in three-dimensional, unsteady flows. Initial steps along this path are presently underway in the Fluid Mechanics Laboratory at NASA Ames. Spectral measurements are being made of the color-change response of liquid crystal coatings beneath surface shear stress vectors of known direction (relative to the observer) and known relative magnitude (see AIAA Paper 94-0729, by Reda and Muratore, Jan. 1994). Such point measurements will ultimately be followed by full-field colorimetric measurements of coating responses to three-dimensional surface shear stress vector fields containing calibration points of known shear magnitude and direction.

## Conclusions

1) For shear-stress-sensitive liquid crystal coatings prealigned by shear into the color-play state and obliquely illuminated by white light, the dispersed (reflected) spectrum was found to be a three-dimensional color space symmetric about the light plane.

2) Under shear, the sense of the angular displacement of the dispersed spectrum relative to a fixed observer was found to be a function of the instantaneous direction of the applied surface shear stress.

3) Since normal-jet impingement simultaneously imposes equal-magnitude shear stress vectors encompassing all possible orientations, it provides a simple method to calibrate the shear-direction response of any liquid crystal coating.

4) In general, to best utilize these characteristics of liquid crystal coatings for flow-direction indication, the principal flow direction(s) should be approximately perpendicular to the light plane, the plane of the observer should be offset (rotated) from the light plane, and the view angle within the observation plane should be at a no-shear/midspectrum orientation. The technique can also be applied to the special case wherein the light, camera, and principal flow direction(s) are all in the same plane (e.g., operation through a single window) with no loss in signal quality.

5) Using this technique, dynamic flow reversals or flow divergences can now be made visible over an entire test surface at image recording rates up to order 1 kHz.

6) Extensions of the technique to visualize relatively small changes in surface shear stress direction appear feasible.

## Acknowledgments

Credit is given to Wade Sisler, Jay Scheibe, Brent Adams, and Tom Reddy of the Imaging Technology Branch, NASA Ames Research Center, for their important contributions in video recording, frame capturing, and video editing. Credit is given to Doug Edwards of Calspan Corporation for his efforts in designing and fabricating the optics-traversing rig. Credit is given to Tim Archer of Breene Kerr Productions, Mountain View, CA, for his creation of the video graphics used herein. And finally, credit is given to Mehran Tadjfar, National Research Council Postdoctoral Fellow at NASA Ames Research Center, for his assistance in the applications of the FAST computer software to current data-analysis and color-imaging needs.

## References

[1]Gray, G. W., *Molecular Structure and the Properties of Liquid Crystals,* Academic Press, New York, 1962.

[2]Fergason, J. L., "Liquid Crystals," *Scientific American,* Vol. 211, No. 8, 1964, pp. 76–85.

[3]Kasagi, N., Moffat, R. J., and Hirata, M., "Liquid Crystals," *Handbook of Flow Visualization,* edited by W. J. Yang, Hemisphere, New York, 1989, Chap. 8, pp. 105–124.

[4]Parsley, M., private communication r.e. Hallcrest liquid crystal mixtures BCN/192, BCN/195, BN/R50C, and CN/R3, Hallcrest, Liquid Crystal Div., Glenview, IL, Aug. 1991.

[5]Terzian, A., private communication r.e. BDH liquid crystal mixtures TI 511 and TI 622, EM Industries, Advanced Chemicals Div., Hawthorne, NY, Sept. 1989.

[6]Klein, E. J., "Liquid Crystals in Aerodynamic Testing," *Astronautics and Aeronautics,* Vol. 6, July 1968, pp. 70–73.

[7]Klein, E. J., and Margozzi, A. P., "Exploratory Investigation on the Measurement of Skin Friction by Means of Liquid Crystals," NASA TM-X-1774, May 1969.

[8]Holmes, B. J., Gall, P. D., Croom, C. C., Manuel, G. S., and Kelliher, W. C., "A New Method for Laminar Boundary Layer Transition Visualization in Flight: Color Changes in Liquid Crystal Coatings," NASA TM-87666, Jan. 1986.

[9]Reda, D. C., "Liquid Crystals for Unsteady Surface Shear Stress Visualization," AIAA Paper 88-3841, July 1988.

[10]Gaudet, L., and Gell, T. G., "Use of Liquid Crystals for Qualitative and Quantitative 2-D Studies of Transition and Skin Friction," Royal Aerospace Establishment, TM AERO-2159, London, June 1989.

[11]Bonnett, P., Jones, T. V., and McDonnell, D. G., "Shear-Stress Measurement in Aerodynamic Testing Using Cholesteric Liquid Crystals," *Liquid Crystals,* Vol. 6, No. 3, 1989, pp. 271–280.

[12]Toy, N., Savory, E., and Paskin, S., "The Development of a System for Real-Time, Full-Field Surface Shear Stress Measurements Using Liquid Crystals," *12th Symposium on Turbulence,* University of Missouri-Rolla, Rolla, MO, Sept. 1990, pp. B15-1–B15-8.

[13]Mee, D. J., Walton, T. W., Harrison, S. B., and Jones, T. V., "A Comparison of Liquid Crystal Techniques for Transition Detection," AIAA Paper 91-0062, Jan. 1991.

[14]Reda, D. C., "Observations of Dynamic Stall Phenomena Using Liquid Crystal Coatings," *AIAA Journal,* Vol. 29, No. 2, 1991, pp. 308–310.

[15]Hall, R. M., Obara, C. J., Carraway, D. L., Johnson, C. B., Wright, E. J., Covell, P. F., and Azzazy, M., "Comparisons of Boundary-Layer Transition Measurement Techniques at Supersonic Mach Numbers," *AIAA Journal,* Vol. 29, No. 6, 1991, pp. 865–871.

[16]Parmar, D. S., "A Novel Technique for Response Function Determination of Shear Sensitive Cholesteric Liquid Crystals for Boundary Layer Investigations," *Review of Scientific Instruments,* Vol. 62, No. 6, 1991, pp.

1596–1608.
[17]Toy, N., Savory, E., and Disimile, P. J., "Determination of Surface Temperature and Surface Shear Stress Using Liquid Crystals," *Forum on Turbulent Flows,* ASME-JSME Joint Fluids Engineering Conference, Portland, OR, June 1991, pp. 39–44.
[18] Reda, D. C., and Aeschliman, D. P., "Liquid Crystal Coatings for Surface Shear-Stress Visualization in Hypersonic Flows," *Journal of Spacecraft and Rockets,* Vol. 29, No. 2, 1992, pp. 155–158.
[19]Smith, S. C., "Use of Shear-Sensitive Liquid Crystals for Surface Flow Visualization," *Journal of Aircraft,* Vol. 29, No. 2, 1992, pp. 289–293.
[20]Wolf, S., Laub, J., King, L., and Reda, D., "Development of NASA-Ames Low-Disturbance Supersonic Wind Tunnel for Transition Research up to Mach 2.5," AIAA Paper 92-3909, July 1992.
[21]Wand, M. D., Vohra, R., O'Callaghan, M., Roberts, B., and Escher, C., "An Easily Aligned Deformable Helix Ferroelectric Liquid Crystal Mixture and its Use in Devices," *Liquid Crystal Materials, Devices, and Applications,* Society of Photo-Optical Instrumentation Engineers, Vol. 1665, Feb. 1992, pp. 176–183.
[22]Murai, H., Gotoh, T., Suzuki, M., Hasegawa, E., and Mizoguchi, K., "Electro-Optic Properties for Liquid Crystal Phase Gratings," *Liquid Crystal Materials, Devices, and Applications,* Society of Photo-Optical Instrumentation Engineers, Vol. 1665, Feb. 1992, pp. 230–239.